Am J Cancer Res 2026;16(3):1027-1041
www.ajcr.us /ISSN:2156-6976/ajcr0163681

Original Article

PIM1 expression is prognostic in clear cell renal cell carcinoma and influenced by an IL-6/JAK/STAT axis

Kimberly S Meza[1,2,3], Kimberly Seymour[2,3], Elias OU Eteshola[2,3], Natalie Payne[2,3], Brianna Rodriguez[2,3], Stephanie L Graff[2,4], Norm Smith[5], Andrew Elliott[5], Wafik S El-Deiry[2,3,4], Sheldon L Holder[2,3,4]

[1]Pathobiology Graduate Program, Brown University, Box G, Providence, RI 02912, USA; [2]Legorreta Cancer Center, Brown University, 70 Ship St, Providence, RI 02903, USA; [3]Department of Pathology and Laboratory Medicine, Brown University, 70 Ship St, Providence, RI 02903, USA; [4]Brown University Health, 110 Lockwood St, Providence, RI 02903, USA; [5]Caris Life Sciences, 750 W John Carpenter Fwy Suite 800, Irving, TX 75039, USA

Received February 3, 2025; Accepted March 2, 2026; Epub March 25, 2026; Published March 30, 2026

Abstract: Renal cell carcinoma (RCC) is among the top ten most common cancers diagnosed in the United States. The incidence of RCC has continued to increase in recent years, yet our understanding of its etiology is incomplete. Clear cell RCC (ccRCC) is the major subtype, constituting over 75% of all RCC cases. Treatment options for RCC are limited in efficacy, as RCC tumors typically acquire resistance to current therapies, particularly in advanced and metastatic RCC. von Hippel-Lindeau (VHL) status is the only clinically validated biomarker approved for therapeutic intervention in RCC to date. The identification of novel molecular targets is therefore critical for improving therapeutic strategies for RCC. PIM1 is a constitutively active serine/threonine kinase involved in promoting proliferation, invasion, migration, and apoptosis evasion in cancer. *PIM1* expression is dysregulated in ccRCC, contributing to oncogenesis and tumor progression. Here, we explore the influence of *PIM1* expression in real-world outcomes of patients with RCC. We identify a link between IL-6 expression and *PIM1* expression and activity in human ccRCC tumors and cell lines. Our work provides evidence that targeting an IL-6/JAK/STAT/PIM1 axis may be a viable therapeutic strategy for patients with *PIM1*-high expressing ccRCC.

Keywords: PIM1 kinase, PIM kinases, IL-6, ruxolitinib, JAK, STAT, renal cell carcinoma

Introduction

In the United States (U.S.), renal cell carcinoma (RCC) is one of the ten most commonly diagnosed cancers for men and women and is estimated to contribute to more than 80,000 new cases and more than 15,00 deaths in 2026 [1, 2]. RCC is also now ranked tenth for most common cancer deaths in men in the U.S. [3]. Trendlines in cancer incidence demonstrate that the number of new cases of RCC has doubled since 1975 and continues to rise steadily [4]. Despite advancements in therapeutic interventions, the five-year overall survival of patients with metastatic RCC is approximately 13% due to acquired resistance to therapy [1]. Thus, investigations into oncogenic and resistance mechanisms of RCC are urgently needed to develop novel clinically relevant treatment strategies.

Clear cell renal cell carcinoma (ccRCC) constitutes the largest subset (approximately 75-80%) of RCC cases [4]. It is a highly heterogeneous and aggressive subtype of tumor that arises from the renal epithelium [2, 5-8]. The most frequently associated genetic alteration for the development of RCC is inactivation of the von Hippel-Lindeau (*VHL*) gene [9]. The *VHL* gene functions as a tumor suppressor, and its dysregulation is a critical factor for Hypoxia Induced Factor 1 alpha (HIF1α) and 2 alpha (HIF2α) to induce the activation of genes and pathways involved in angiogenesis, cell cycle progression, cell proliferation, and metabolism [9]. VHL inactivation is a driver of RCC carcinogenesis and is observed in up to 90% of patients with ccRCC, whether via sporadic or inherited VHL inactivation [2, 6, 9]. At present, VHL disease is the only clinically validated biomarker for RCC treatment [10].

https://doi.org/10.62347/LQQL3584

Standard therapy for metastatic RCC includes immune checkpoint inhibitors and antiangiogenic agents (mostly targeting vascular endothelial growth factor (VEGF) or mammalian target of (mTOR) signaling) [2, 7, 8, 11-13]. Unfortunately, acquired resistance to current therapies is almost inevitable and underscores the importance of investigating and establishing novel actionable biomarkers for the treatment of RCC [14-17].

Overexpression of proviral integration site for Moloney murine leukemia virus 1 (*PIM1*) kinase is correlated with poor patient prognosis and clinical outcomes across many cancers, including RCC [18-29]. As an oncoprotein, PIM1 phosphorylates a diverse body of substrates with key roles in cancer processes [21-34]. To sustain proliferative signaling, PIM1 can target Cyclin-dependent kinase inhibitor 1A (p21/WAF1), Cyclin-dependent kinase inhibitor 1B (p27/KIP1), and cellular myelocytomatosis oncogene (c-myc). It can also promote cell survival via directly phosphorylating BCL2 associated agonist of cell death (BAD), and Forkhead Box O3 (FOXO3a) in addition to enabling cell migration through C-X-C motif chemokine receptor 4 (CXCR4), among others [30, 33]. In RCC, PIM1 was found to promote carcinogenesis by influencing cell proliferation, colony formation, migration, invasion, and angiogenesis [18-20]. PIM1 also mediates epithelial-mesenchymal transition (EMT) in RCC via interaction with and phosphorylation of Suppressor of Mothers against Decapentaplegic 2 (Smad2) or 3 (Smad3) [20]. We have shown that PIM1 protein levels are increased in RCC compared to normal adjacent tissue [19]. Moreover, we and others have demonstrated that using PIM1 inhibitors alone or in combination with VEGF inhibitors leads to a synergistic reduction in tumor burden, decreased RCC cell viability, and increased apoptosis, thus establishing PIM1 as an attractive target in RCC [17-19]. However, the mechanisms that underlie *PIM1* expression and its regulation in RCC remain to be elucidated.

Wild-type PIM1 is constitutively active [25-28]. Phosphorylation is not necessary for mediating its catalytic activity but may serve to stabilize the protein [35]. Thus, protein levels are indicative of PIM1 activity. Many factors influence *PIM1* expression and protein levels, including nuclear factor kappa-light-chain-enhancer of activated B (NF-κB), krueppel-like factor 5 (KLF5), and heat shock protein (HSP) 90 (HSP90) and (HSP70) which regulate PIM1 transcriptionally or impact protein stabilization [20, 30, 32]. Signal transducers and activators of transcription (STAT) 3 and 5 (downstream of janus kinase (JAK)) bind to the promoter region of *PIM1*, transcriptionally upregulating PIM1 in response to stimuli from growth factors, mitogens, and cytokines [21, 23, 32, 36-38]. One such cytokine is interleukin 6 (IL-6) [39, 40]. IL-6 is a pleiotropic protumorigenic cytokine that signals through the JAK/STAT pathway, and high serum IL-6 levels are associated with worse patient outcomes in patients with RCC [41, 42]. Here, we report that an IL-6/JAK/STAT/PIM1 pathway is active in RCC. A similar IL-6/JAK/STAT/PIM1 pathway has been reported in pancreatic cancer and breast cancer [39, 40]. We demonstrate that RCC cells secrete IL-6 and that targeting an IL-6/JAK/STAT axis in RCC modulates PIM1 kinase activity [43, 44]. Additionally, we explore the influence of PIM1 on clinical outcomes in a large cohort of real-world patients with RCC.

Materials and methods

Patient study cohorts

TCGA cohort: Survival analysis of *PIM1* high ccRCC patients was conducted using The Cancer Genome Atlas (TCGA, Firehose Legacy, Kidney Renal Clear Cell Carcinoma) in cBioPortal [45, 46]. Comparisons of PIM1 in normal tissue and clear cell renal cell carcinoma by stage, grade, and subtype was evaluated using the UALCAN data analysis platform [47, 48].

Atlas of the plasma proteome: Atlas of the Plasma Proteome was assessed for IL-6 plasma levels in cases of malignant neoplasm of the kidney (N = 211), excluding renal pelvis. Healthy controls exclude all cancers [49].

Caris cohort: The study cohort included real-world patients with a kidney cancer diagnosis (N = 1166) with formalin-fixed paraffin-embedded (FFPE) tissue samples submitted to a commercial CLIA-certified laboratory for molecular profiling (Caris Life Sciences, Phoenix, AZ, USA). This study was conducted in accordance with guidelines of the Declaration of Helsinki, Belmont report, and U.S. Common rule. In keeping with 45 CFR 46.101(b)(4), this study

was performed utilizing retrospective, deidentified clinical data. Therefore, the study was deemed Institutional Review Board exempt, and no patient consent was necessary from the subjects.

DNA/RNA next-generation sequencing

Microdissection was performed prior to sequencing to facilitate the enrichment of tumor content. Next-generation sequencing was performed on isolated genomic DNA using the NextSeq platform (Illumina, Inc., San Diego, CA, USA) for a targeted panel of 592-720 cancer-relevant genes (N = 175 samples) or the Illumina NovaSeq 6000 platform (Illumina, Inc., San Diego, CA, USA) for whole-exome sequencing (N = 991 samples). Whole-transcriptome sequencing used a hybrid-capture method to pull down the full transcriptome from FFPE tumor samples (N = 1166) using the Agilent SureSelect Human All Exon V7 bait panel (Agilent Technologies, Santa Clara, CA, USA) and the Illumina NovaSeq platform (Illumina, Inc.). Genomic variants were classified by board-certified molecular geneticists according to criteria established by the American College of Medical Genetics and Genomics. When assessing mutation frequencies of individual genes, 'pathogenic' and 'likely pathogenic' variants were counted as mutations, while 'benign' and 'likely benign' variants and 'variants of unknown significance' were excluded.

Gene expression profiling/pathway analysis

Gene set enrichment analysis (GSEA) was performed using pre-ranked gene lists based on the median fold-change between *PIM1*-high and *PIM1*-low samples to examine the Molecular Signatures Database (MSigDB) hallmark gene set collection [50, 51]. The top 500 genes with increased expression in *PIM1*-high samples were further analyzed for pathway enrichment using gProfiler to assess Gene Ontology (GO), Kyoto Encyclopedia of Genes and Genomes (KEGG), and Reactome gene set collections [52].

Survival analysis

Kaplan-Meier survival analysis was used to assess clinical outcomes from insurance claims data. Survival was calculated from the initial diagnosis date, specimen collection date, or treatment start date until the last clinical contact date or death. Metastatic tumors were classified based on review of the specimen biopsy sites, in which patients with a specimen biopsy site distant from kidney were classified as 'metastatic', while those with a specimen biopsy site of kidney were considered 'kidney'. Cox proportional hazard ratios were calculated for each comparison group, with *P*-values calculated using the log-rank test.

Statistical analysis and data visualization

Statistical analyses were performed using the python packages Pandas, NumPy, and SciPy. Continuous data were assessed using a Mann-Whitney U test, and categorical data were evaluated using Chi-square or Fisher's exact test, where appropriate.

Cell lines

Renal cell lines, HK-2, RPTEC, CAKI-1, ACHN, 769-P and 786-O were purchased from American Type Culture Collection (ATCC). RCC-4 were gifted from Wafik El-Deiry. HK-2 were cultured in DMEM F-12 (Gibco) supplemented with 10% fetal bovine serum (FBS) and 1% penicillin streptomycin. RPTEC were cultured in Renal epithelial cell basal medium (ATCC) supplemented with Renal epithelial cell growth kit (ATCC). CAKI-1 were cultured in McCoy's (Corning) supplemented with 10% FBS and 1% penicillin streptomycin. ACHN and RCC-4 were cultured in DMEM (Gibco) supplemented with 10% FBS and 1% penicillin streptomycin. 769-P and 786-O were cultured in RPMI (Gibco) supplemented with 10% FBS and 1% penicillin streptomycin. Cells were cultured following the manufacturer's protocol and incubated at 37°C in a 5% CO_2 incubator.

Immunoblotting assay

Cells were lysed with RIPA buffer (Thermo Scientific, 89901) supplemented with protease and phosphatase inhibitors (Thermo Scientific, A32953, A32957) according to manufacturer's instruction. Protein concentrations were determined using the Pierce BCA protein assay kit (23225, Thermo Scientific). Standardized amounts of proteins were resolved by SDS-PAGE and then transferred to PVDF membranes. Membranes were pre-wetted with methanol. Membranes were blocked with 5%

non-fat powdered milk or 3% bovine serum albumin in tris-buffered saline (TBS) for 1 hour at room temperature.

Anti-phospho JAK2 (1:1000 dilution, Invitrogen PA5-85735), Anti-JAK2 (1:1000 dilution, Invitrogen AH01352), Anti-phospho STAT3 (1:1000, Cell Signaling 9131), Anti-Stat3 (1:1000, Cell Signaling 9139), Anti-PIM1 (1:1000 dilution, Abclonal A19695), anti-β-Actin (1:5000 dilution, Sigma-Aldrich A5441) were used as the primary antibodies. Membranes were incubated with the specific primary antibody at 4°C overnight and then washed with TBS with 0.1% Tween® 20 (TBST) before incubating with secondary anti-rabbit IgG, HRP-linked antibody (Cell Signaling Technology, 7074) or anti-mouse IgG, HRP-linked antibody (Cell Signaling Technology, 7076) at room temperature for 1 hour. The target protein band was then visualized using ECL and West Femto western blot detection substrates (Thermo Scientific, 32106, 34095) on the Genesys system (Syngene).

IL-6 enzyme linked immunosorbent assay (ELISA)

Cells were plated on a 6-well plate at 200,000 cells/well in triplicate. After cells adhered overnight, media was removed, and fresh media was added to each well. After 24 hours, cell conditioned media was collected and centrifuged to remove any particulate material. Concentration of IL-6 was detected using the Human IL-6 ELISA KIT II (BD Biosciences, 550799) according to the manufacturer's protocol.

Ruxolitinib treatment

For the experiment detecting protein levels after treatment, cells were seeded on a 6-well plate at a density of 500,000 cells/well to adhere overnight. The following day, cell media was removed from the wells and replaced with fresh media containing the indicated concentrations of ruxolitinib (MedChemExpress, HY-50856) and incubated for 8 hours. Cells were then prepared for protein harvest as described in the immunoblotting methods. The following additional antibodies were used in the time course blot: Anti-phospho-BAD (1:1000, Cell Signaling 9291), Anti-BAD (1:1000, Cell Signaling 9292), Anti-phospho Foxo3a (1:1000, Cell Signaling 9466), Anti-Foxo3a (1:1000, Cell Signaling 2497) and Anti-p27/Kip1 (1:0000, Cell Signaling 9552).

Real-time PCR (qRT-PCR) assay

Total RNA was extracted from treated cell pellets using an RNA miniprep kit (Qiagen, #74104). Total RNA was quantified and checked for purity, and 1 ug was used to prepare 20 µl of cDNA with an iScript cDNA Synthesis Kit (Bio-Rad, 170-8891). Real-time PCR was performed in technical triplicate using DNA template, ABI SYBR green PCR master-mix (Applied Biosystems, A25742), and custom oligos (Invitrogen) for Pim1 and 18s rRNA in a 20 µl reaction on an Applied Biosystems QuantStudio 6 Pro Real-Time PCR System. Data were analyzed by the ΔΔCt method, and relative expression levels were normalized to 18s rRNA. Primer sequences are Pim1: For-CTGCTCAAGGACACCGTCTACA, Rev-GATGGTAGCGGATCCACTCTTG and 18s: For-CCGCGGTTCTATTTTGTTGG, Rev-GGCGCTCCCTCTTAATCATCATG.

Immunocytochemistry

To detect intracellular protein levels of PIM1 kinase, 786-0 cells were plated in a 8-well chamber glass slide at a density of 30,000 cells/well to attach overnight. The following day, media was removed and replaced with 300 µL of media with indicated doses of ruxolitinib or DMSO vehicle control. After 8 hour treatment, media was removed from wells and rinsed with PBS. Cells were fixed with 4% paraformaldehyde (PFA) for 20 minutes at room temperature (RT). After incubation with PFA, wells were rinsed with PBS and permeabilized with 0.1% Triton X in PBS for 15 minutes. Endogenous peroxidases were blocked using 3% H_2O_2. Blocking was performed using 2.5% Horse serum for 30 minutes at RT (Vector Laboratories, MP-7401). Chamber was removed and primary Anti-PIM1 (1:250, Abclonal A19695) was added to each well (except for controls, which did not receive any primary antibody) for overnight incubation. Secondary Anti-Rabbit IgG (Vector Laboratories, MP-7401) was added to each well for 30 minutes at RT. DAB substrate was prepared according to manufacturer (Vector Laboratories, SK-4100) and added to each well until color change was observed under brightfield microscope. Slide was rinsed with distilled H_2O, counterstained with Haematoxylin for 5 minutes, and briefly

rinsed in 1% hydrochloric acid in 75% ethanol. Following a rinse in H_2O, slide was dehydrated in increasing ethanol concentrations and xylenes. Slide was mounted with Cytoseal XYL and imaged.

Synergy assay

Cells were plated at a density of 3,000 cells/well in an opaque walled 96 well plate and incubated overnight in 100 µL media at 37°C in a 5% CO_2 incubator. The following day, an additional 20 µL of treated or vehicle control (DMSO) media was added to the indicated well following serial 2 fold dilution of the drug at the initial concentration. At 72 hours treatment, 20 µL of CellTiterGlo reagent (Promega Corporation) was added to each treatment and control well containing 120 µL media and shaken on an orbital shaker for approximately 2 minutes. Cell viability was determined using CTG bioluminescent imaging on a Xenogen IVIS imager. Normalization of luminescence signals to control wells determined percent cell viability. Results are reported as percent inhibition. The expected drug combination responses were calculated based on HSA reference model using SynergyFinder [53]. Synergy scores were calculated using SynergyFinder+ web application [54]. Deviations between observed and expected responses with positive and negative values denote synergy and antagonism respectively.

Results

PIM1 is elevated in RCC tumors relative to tumor stage, grade, and risk subtype

PIM1 overexpression is associated with poor clinical outcomes in many cancers [23, 24, 32]. To understand the role of *PIM1* expression in RCC outcomes, we conducted analyses of clinically relevant pathologic factors in a published database, The Cancer Genome Atlas (TCGA) using the UALCAN integrated portal [47, 48]. Here, we find that high *PIM1* expression (> median transcripts per million (TPM)) in ccRCC tumors demonstrate significantly worse overall survival (OS) than *PIM1* low (< median TPM) ccRCC tumors (HR = 2.230, 95% CI: 1.657-3.001, P<0.0001, **Figure 1A**). Additionally, *PIM1* expression is significantly increased in stage 4 disease compared to stage 1 disease, with increasing expression trends across stages (P = 0.04, **Figure 1B**). Relative to tumor grade, *PIM1* expression is also increased in grade 4 tumors compared to normal tissue (P<0.05) as well as grade 1 (P<0.05) or grade 2 tumors (P<0.05, **Figure 1C**), with a trend towards increasing *PIM1* across tumor grades. In analyses of prognostic subtypes, we also find that *PIM1* expression is significantly elevated in 'poor risk' ccB subtype tumors compared to 'good risk' ccA subtype ccRCC tumors (P<0.0001, **Figure 1D**) [55]. In summary, we find that expression of *PIM1* is significantly elevated in ccRCC tumors, corresponding to worse survival and tumor attributes.

High PIM1 expression is prognostic for poor survival in patients with RCC

To better understand the prognostic influence of *PIM1* in RCC, we also investigated *PIM1* expression in tumor samples from 1166 real-world patients with RCC from an independent genomics database (Caris cohort). In the most common RCC subtype, ccRCC, patients whose tumors had high median *PIM1* expression show a statistically significant shorter OS relative to patients whose tumors had low median *PIM1* expression. The OS difference is significant whether measured from the date of tissue sample collection (HR = 1.607, 95% CI: 1.264-2.042, P<0.0001, **Figure 2A**) or the date of first diagnosis (HR = 1.64, 95% CI: 1.267-2.122, P<0.001, **Figure 2B**). The median OS of patients with *PIM1*-high ccRCC and *PIM1*-low RCC is 72.9 and 45.7 months, respectively (**Figure 2A**).

Interestingly, high PIM1 expression is not associated with survival in papillary RCC (HR = 1.011, 95% CI: 0.616-1.657, P = 0.968, **Figure 2C**) or chromophobe RCC (HR = 1.71, 95% CI: 0.446-3.074, P = 0.748, **Figure 2D**). In sarcomatoid RCC, *PIM1* expression trends towards worse OS but does not reach statistical significance (HR = 1.651, 95% CI: 0931-2.926, P = 0.082, **Figure 2E**).

We also evaluated *PIM1* expression in primary versus metastatic tumors within each RCC subtype. In ccRCC, median *PIM1* expression is higher in metastatic tumors compared to primary tumors (6.44 TPM and 5.18 TPM, respectively, P<0.0001). Similarly, sarcomatoid RCC metastatic tumors have increased median *PIM1* expression relative to primary tumors (13.85 TPM and 7.57 TPM, P<0.01). However, in papillary RCC there is no statistically signifi-

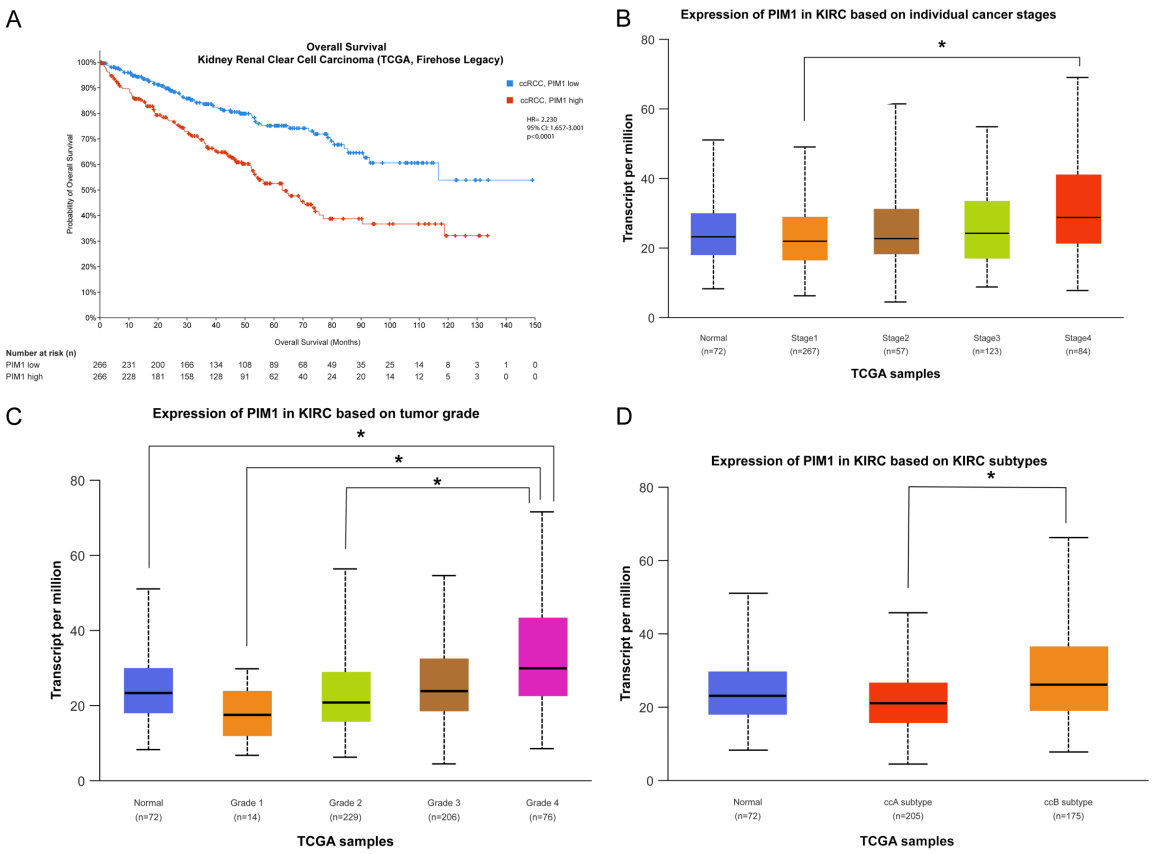

Figure 1. *PIM1* is elevated in RCC tumors relative to tumor stage, grade and risk subtype. High *PIM1* (> median TPM) is associated with worse OS in ccRCC patients from The Cancer Genome Atlas (TCGA, ccRCC, Firehose Legacy) (P<0.0001) (A). *PIM1* expression is increased in ccRCC stage 4 tumors compared to stage 1 (P = 0.04) (B). PIM1 expression is greater in grade 4 tumors relative to normal tissue (P = 0.046), grade 1 (P = 0.023), grade 2 (P = 0.024) (C). In cRCC subtypes, *PIM1* was significantly higher in worse risk subtype ccB than ccA (P<0.0001) (D).

cant difference in *PIM1* expression based on the site of disease (metastatic tumors, 6.19 TPM vs primary tumors, 5.09 TPM, P = 0.059), and in chromophobe RCC median *PIM1* expression is lower in metastatic tumors (9.24 TPM) compared to primary tumors (13.56 TPM, P = 0.015) (**Figure 2F**).

These results indicate that *PIM1* overexpression is associated with poor prognosis in patients with ccRCC and potentially also sarcomatoid RCC.

IL-6 signaling correlates with PIM1 expression in ccRCC

IL-6 is an activating cytokine of the JAK/STAT signaling cascade and is reported to influence *PIM1* expression in pancreatic and breast cancer [39, 40]. We therefore investigated whether this signaling axis may exist in RCC. We interrogated a comprehensive plasma proteome database, The Atlas of Plasma Proteome Linking to Health and Disease, and found that upregulation of IL-6 was significantly associated with the incidence of malignant neoplasms of the kidney compared to healthy controls (HR = 1.17, 95% CI: 1.02-1.35, P<0.05, **Figure 3A**) [49]. We then examined tumors from 875 real-world patients with ccRCC (Caris cohort) to determine whether *IL-6* expression is related to *PIM1* expression. We found that median *IL-6* expression was 3.27-fold greater in *PIM1*-high ccRCC tumors (4.79 TPM) than in *PIM1*-low ccRCC tumors (1.46 TPM), indicating that *IL-6* expression is significantly correlated with *PIM1* expression (Spearman rank correlation ρ = 0.414, P<0.001) (**Figure 3B**). Next, we performed pathway analyses of differentially expressed genes (DEGs) using gene set enrichment analysis (GSEA) and identify that *PIM1*-high ccRCC tumors exhibit increased inflammatory signa-

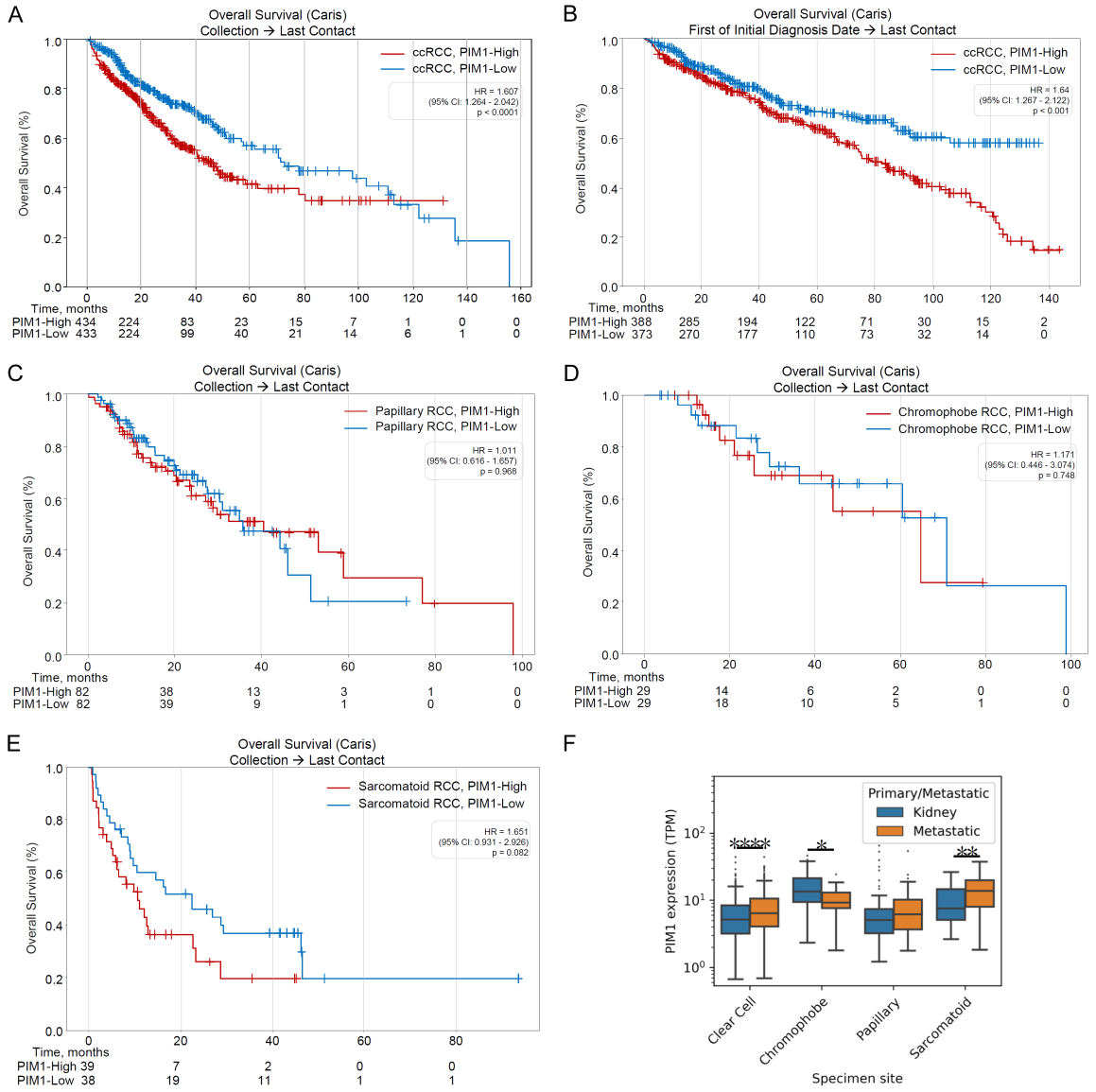

Figure 2. High *PIM1* expression is prognostic for poor survival in patients with RCC. High *PIM1* (> median TPM) is associated with worse OS in ccRCC patients, as measured from the date of first sample collection (P<0.0001) (A) or first diagnosis (P<0.001, ****P) (B). High PIM1 expression is not associated with survival in papillary RCC (P = 0.968) (C) or chromophobe RCC (P = 0.748) (D) but trends towards worse OS in sarcomatoid RCC (P = 0.082) (E). *PIM1* expression is 1.24-fold significantly increased in metastatic ccRCC tumors (median = 6.44 TPM, N = 390) relative to primary (median = 5.18 TPM, N = 485, P<0.000003, ****P). *PIM1* expression is decreased in metastatic chromophobe RCC (median = 9.24 TPM, N = 20, P = 0.015, *P) compared to primary chromophobe RCC (median = 13.56 TPM, N = 39). *PIM1* expression does not differ in primary papillary RCC tumors (median = 5.09 TPM, n = 118) relative to metastatic papillary RCC tumors (median = 6.19 TPM, N = 47, P = 0.059). *PIM1* expression is significantly increased in metastatic sarcomatoid RCC tumors (median = 13.85 TPM, N = 39) compared with primary sarcomatoid RCC tumors (median = 7.57 TPM, N = 38, P = 0.007, **P) (F).

tures, including upregulation of tumor necrosis factor alpha (*TNFα*), EMT and IL-6/JAK/STAT3 signaling (**Figure 3C-E**). In each of these, *IL-6* is among the top two DEGs associated with the signature (**Figure 3C-E**). *PIM1* appears as the top fourth ranked DEG in the IL-6/JAK/STAT3 signaling plot (**Figure 3C**). Furthermore, based on the Gene Ontology (GO) pathway gene sets, *PIM1*-high ccRCC tumors are associated with the upregulation of immune-related genes, such as genes related to cytokine receptor binding and immune system processes (**Figure**

A

Atlas of Plasma Proteome

Protein	N	HR [95% CI]	p - value
IL-6	211	1.17 [1.02-1.35]	0.0204

B

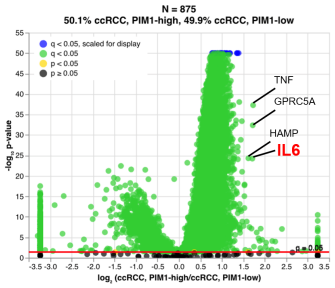

C

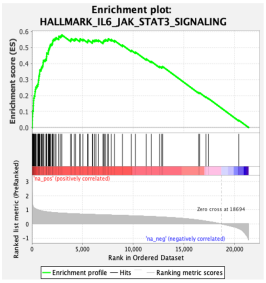

	SYMBOL	RANK IN GENE LIST	RANK METRIC SCORE	RUNNING ES
1	TNF	46	1.727	0.0223
2	IL6	48	1.709	0.0464
3	PF4	54	1.529	0.0678
4	PIM1	72	1.389	0.0866
5	PLA2G2A	90	1.313	0.1044
6	CXCL10	146	1.206	0.1188
7	IL1B	147	1.205	0.1359
8	CXCL1	160	1.194	0.1522
9	CCR1	165	1.190	0.1688
10	CD14	186	1.169	0.1844

D

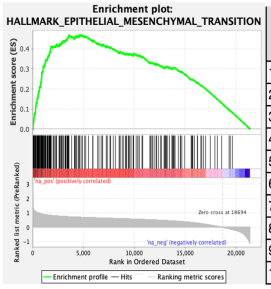

	SYMBOL	RANK IN GENE LIST	RANK METRIC SCORE	RUNNING ES
1	IL6	48	1.709	0.0100
2	COL11A1	59	1.477	0.0201
3	PLAUR	79	1.357	0.0289
4	GREM1	92	1.309	0.0377
5	TGFBI	124	1.240	0.0451
6	PRRX1	145	1.207	0.0529
7	CXCL1	160	1.194	0.0607
8	DCN	177	1.178	0.0684
9	LRRC15	182	1.174	0.0767
10	COL6A3	247	1.124	0.0817

E

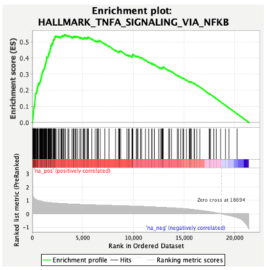

	SYMBOL	RANK IN GENE LIST	RANK METRIC SCORE	RUNNING ES
1	TNF	46	1.727	0.0095
2	IL6	48	1.709	0.0211
3	BCL2A1	70	1.405	0.0296
4	PLAUR	79	1.357	0.0385
5	CCL2	86	1.330	0.0472
6	LIF	107	1.267	0.0549
7	PTGS2	121	1.249	0.0627
8	FOSL1	136	1.215	0.0703
9	CXCL10	146	1.206	0.0780
10	IL1B	147	1.205	0.0862

F

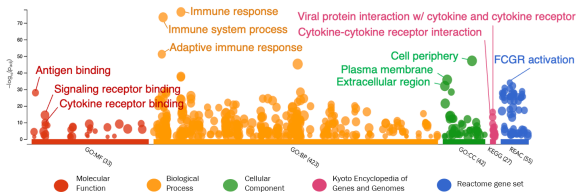

Figure 3. IL-6 signaling influences PIM1 expression in clear cell RCC. Plasma levels of IL-6 is significantly associated with incidence of malignant neoplasms of the kidney relative to healthy controls of Atlas of Plasma Proteome (A). *IL-6* expression is 3.27-fold greater in *PIM1*-high (> median TPM) ccRCC patients than in *PIM1*-low ccRCC patients (< median TPM) (B). *IL-6* is upregulated across the top DEGs and is associated with *TNFα*, EMT, and IL-6/JAK/STAT signatures in *PIM1*-high tumors (C-E). GO analysis reveals that *PIM1*-high tumors have upregulated immune-related profiles (F).

3F). Collectively, these results suggest that *PIM1* expression is closely linked to *IL-6* expression in ccRCC tumors.

JAK inhibition regulates PIM1 expression in human ccRCC cell lines

To further elucidate the influence of IL-6 on *PIM1* expression in ccRCC we investigated a panel of five human ccRCC cell lines (769-P, 786-O, ACHN, CAKI-1, and RCC-4) and two non-malignant renal proximal tubule epithelial cell lines (HK-2 and RPTEC) to determine relative JAK, STAT, and PIM1 protein levels via immunoblotting. We find that among all the ccRCC cell lines, PIM1 protein levels are increased relative to nonmalignant renal epithelial cell lines (**Figure 4A**). Additionally, 786-O, ACHN, and CAKI-1 RCC cells secrete high levels of soluble IL-6 into their media. 769-P cells secrete a negligible concentration of IL-6 (**Figure 4B**). To understand if an IL-6/JAK/STAT axis contributes to PIM1 regulation in ccRCC, we used ruxolitinib, a JAK1/2 inhibitor, to assess the effect on *PIM1* expression and protein levels. Our data show that ruxolitinib is sufficient to decrease PIM1 protein levels in 786-O cells, with a corresponding expected decrease in upstream phosphorylated STAT3 (pSTAT3). In contrast, PIM1 protein levels are not decreased in 769-P cells when treated with ruxolitinib, likely indicating a JAK-independent mechanism is regulating *PIM1* expression in 769-P cells (**Figure 4C**). In 786-O cells, we verified via quantitative reverse transcription polymerase chain reaction (qRT-PCR) that treatment with ruxolitinib decreases *PIM1* messenger ribonucleic acid (mRNA) levels, indicating that this

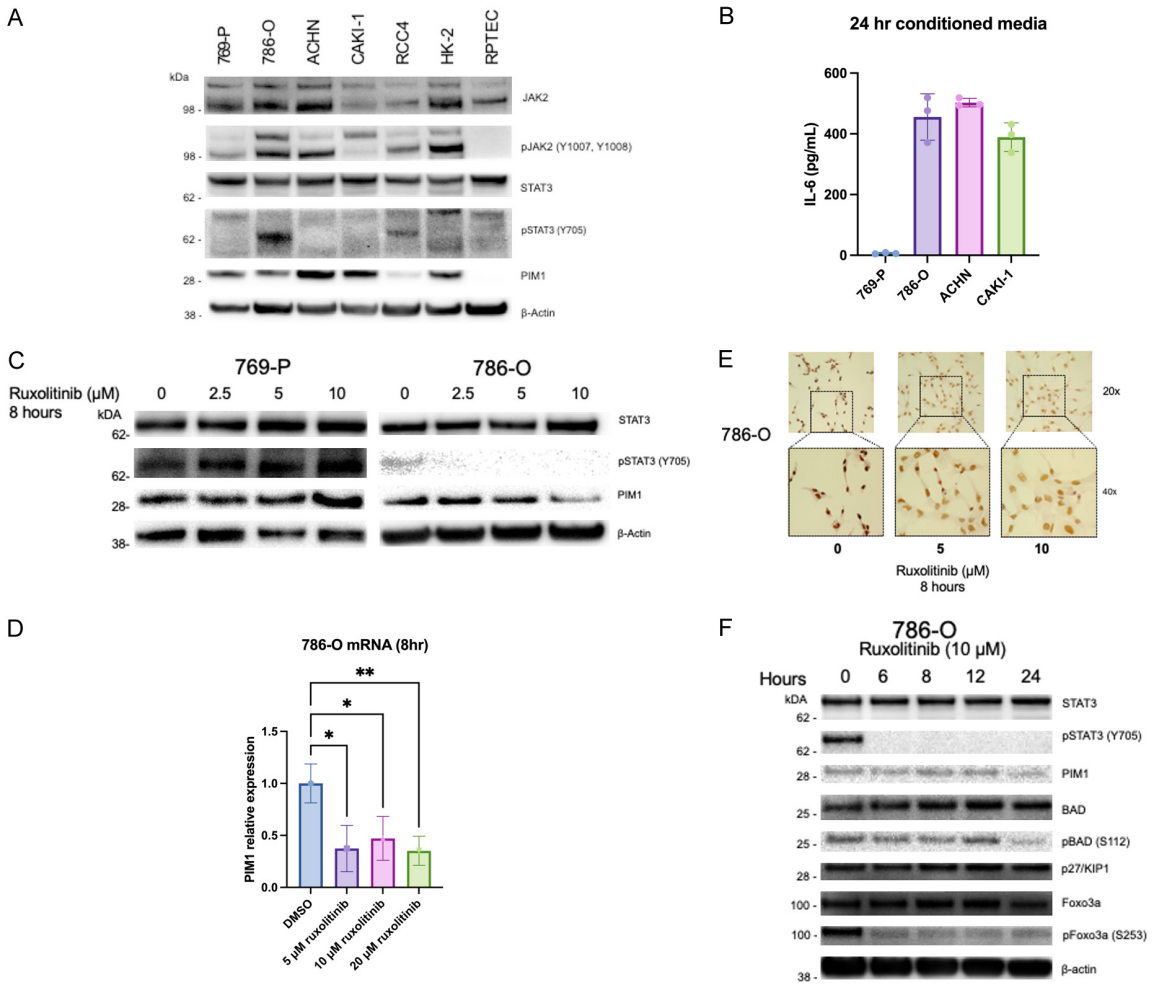

Figure 4. JAK inhibition regulates PIM1 expression in human ccRCC cell lines. Baseline PIM1 protein levels are increased in ccRCC cell lines relative to nonmalignant renal proximal tubule cell lines (A). Soluble IL-6 is detected in 24-hour conditioned media from ccRCC cell lines, except in the 769-P cell line (B). Treatment with ruxolitinib for 8 hours results in a dose-dependent decrease in PIM1 protein in 786-O cells but not in 769-P cells (C). Treatment with ruxolitinib decreases *PIM1* expression in 786-O cells (*P<0.05, **P<0.01) (D). 8 hour treatment with ruxolitinib reduces PIM1 protein detected by immunocytochemistry. Upper Panel - 20X magnification, Lower Panel - 40X magnification (E). 24 hour treatment with 10 μM ruxolitinib in 786-O cells shows decreases in PIM1 substrates pBAD, pFoxo3a, and increasing p27 protein levels as PIM1 protein is reduced (F).

effect occurs transcriptionally to regulate *PIM1* expression (**Figure 4D**). Treatment of 786-O cells with ruxolitinib also decreases PIM1 protein detected via immunocytochemistry (**Figure 4E**). We further evaluated the effect of ruxolitinib on protein levels of phosphorylated BAD (pBAD) [56], phosphorylated Foxo3a (pFoxo3a), and p27/KIP1 [57], downstream targets of PIM1 kinase that promote apoptosis and cell cycle inhibition, respectively. In immunoblotting, we found that ruxolitinib treatment over time modulates PIM1 substrates by gradually reducing its phosphorylated targets; pBAD at Serine 112 and pFoxo3a at Ser253. PIM1 target p27/KIP1, which function as a tumor suppressor, increases in response to ruxolitinib treatment (**Figure 4F**). Taken together, these data support that PIM1 kinase is aberrantly overexpressed in human ccRCC tumors and cell lines and is linked to active IL-6/JAK/STAT signaling. Additionally, *PIM1* expression and PIM1 substrates may be attenuated via upstream JAK inhibition.

Indirect and direct PIM inhibitors exert synergy when used in combination with VEGF inhibition in 786-O cells

To examine the effects of combining upstream or direct targeting of PIM1 with a standard ther-

apy for ccRCC, we performed synergy assays using increasing doses of ruxolitinib, first generation pan PIM inhibitor SGI-1776, or second generation pan PIM inhibitor nuvisertib (TP-3654) and cabozantinib, a VEGF inhibitor, in 786-0 cells. In this study, we used the Highest Single Agent (HSA) model to evaluate synergistic effects of these combinations. We find that the combination of ruxolitinib with cabozantinib is synergistic (score >10) to potently reduce cell viability in 786-0 cells across multiple doses (**Figure 5A**). Similarly, SGI-1776 and TP-3654 also show synergy with cabozantinib across multiple doses. (**Figure 5B**, **5C**). Together, these data suggest that the use of treatment strategies that target PIM1 in combination with VEGF directed therapy may improve upon single agent therapy in ccRCC.

Discussion

The incidence of RCC is on the rise, and the almost invariable development of acquired resistance to current standard-of-care therapies necessitates the identification of novel biomarkers and therapeutic targets to improve the treatment landscape. PIM1 kinase is a promising target for RCC therapy [18-20]. Here, we describe the overexpression of *PIM1* as a prognostic marker for poor clinical outcomes in patients with ccRCC. We show with real-world data that *PIM1* expression is significantly increased in ccRCC tumors by stage, grade, and in metastatic versus primary ccRCC tumors. We also identify that among ccRCC subtypes, high *PIM1* expression is associated with the ccB 'poor risk' subtype and thus indicative of a more aggressive phenotype, corresponding with worse response to antiangiogenic treatments, and more enriched immune and inflammatory gene signatures [55]. Importantly, we show that patients with *PIM1*-high ccRCC patients face worse survival outcomes than their *PIM1*-low counterparts across two independent genomics databases. Current ccRCC therapies do not target PIM1, thus our findings suggest that novel therapeutic agents in ccRCC should target PIM1 or focus on oncogenic pathways that influence PIM1 activity to improve patient outcomes.

Importantly, the influence of *PIM1* on clinical outcomes in RCC is subtype-specific, not just a general association. Increased *PIM1* expression leads to poorer survival in ccRCC. This association holds true whether assessed from the date the sample was collected or from the date of initial diagnosis. In contrast, we did not observe any significant association between *PIM1* expression and survival in papillary or chromophobe RCC. This confirms that papillary and chromophobe subtypes in RCC are disparate entities with distinct molecular and genetic features that likely do not rely on PIM1 oncogenic mechanisms. While *PIM1* expression is higher in metastatic ccRCC than in primary tumors, we did not observe differences in *PIM1* expression between primary versus metastatic tumors in papillary RCC or chromophobe RCC. These data show the effect of PIM1 activity to be selective among RCC subtypes.

Our findings provide evidence that *PIM1* expression plays a significant role in ccRCC. This study reveals a compelling link between elevated *PIM1* and *IL-6* expression in human ccRCC cell lines and in large, real-world patient cohorts. Elevated plasma IL-6 is associated with the incidence of malignant kidney neoplasms. Upon further interrogating *PIM1* high ccRCC tumors, we find that increased *PIM1* expression correlates with increased *IL-6* expression and upregulation of immune and inflammatory signatures and processes in ccRCC tumors, further supporting a relationship with *IL6* expression and *PIM1* expression.

Our work highlights ruxolitinib as an indirect PIM1 inhibitor in RCC cells that downregulates pSTAT3 and PIM1 protein levels with changes observed in the downstream substrates of PIM1. These PIM1 targets such as pBAD and pFoxo3a have crucial roles in promoting apoptosis and are inactivated by PIM1 phosphorylation [56, 57]. We find that ruxolitinib treatment gradually modulates their phosphorylation levels at PIM1 target sites and promotes increased p27/KIP1, a substrate that when downregulated by PIM1 phosphorylation, prevents cell cycle inhibition [57].

The existence of an IL-6/JAK/STAT/PIM1 signaling axis in ccRCC presents a novel viable therapeutic strategy for targeting PIM1 in ccRCC. Several FDA approved agents are clinically available that modulate IL-6 signaling, including agents that directly bind IL-6 (siltuximab) or the IL-6 receptor (tocilizumab), or antagonize JAK (ruxolitinib) (**Figure 6**). These agents could be evaluated in clinical trials in patients with *PIM1*

A

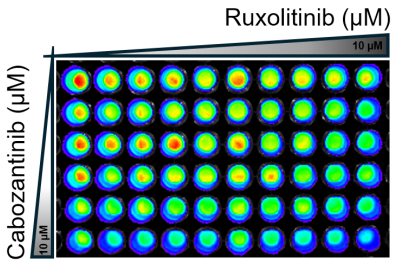

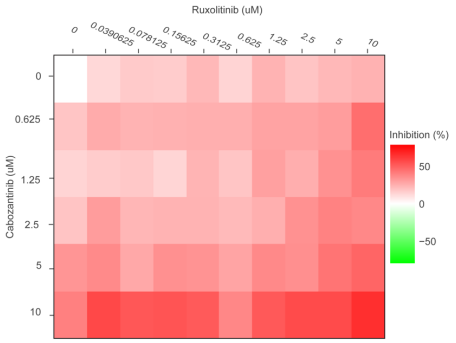

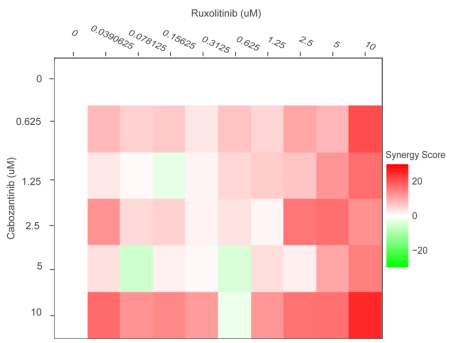

Ruxolitinib (μM)	Cabozantinib (μM)	Synergy Score
10	10	25.46
10	0.625	21.06
0.0390625	10	17.51
10	1.25	17.02
5	2.5	16.97
5	10	16.66
2.5	10	16.56
2.5	2.5	16.12
10	5	15.01
0.15625	10	13.83
10	2.5	13.00
0.0390625	2.5	12.82
0.078125	10	12.80
5	1.25	12.36
1.25	10	12.23
0.3125	10	11.77
5	5	10.50
2.5	0.625	10.32

B

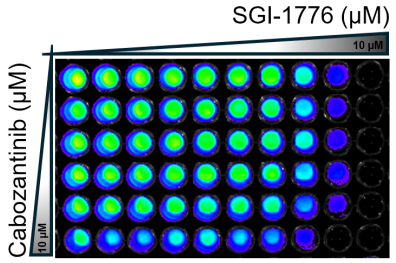

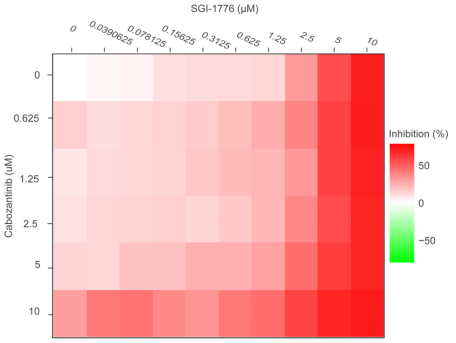

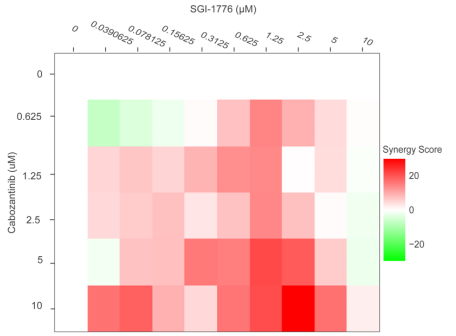

SGI-1776 (μM)	Cabozantinib (μM)	Synergy Score
2.5	10	37.21
1.25	5	21.38
1.25	10	21.00
2.5	5	19.34
0.078125	10	18.70
5	10	16.76
0.0390625	10	16.60
0.625	10	16.39
0.3125	5	15.72
0.625	5	15.14
1.25	0.625	14.50
1.25	2.5	14.09
1.25	1.25	14.00
0.625	1.25	13.24

C

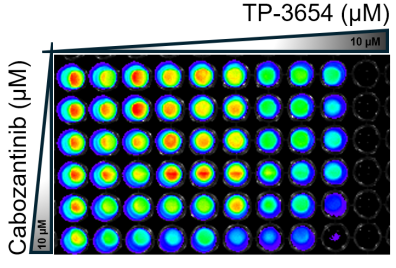

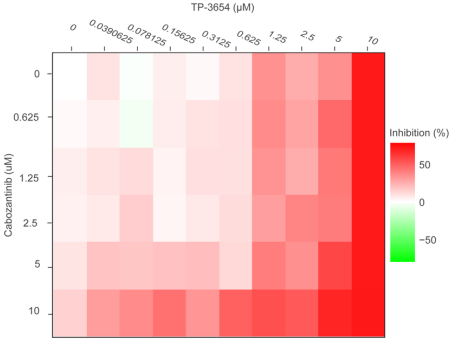

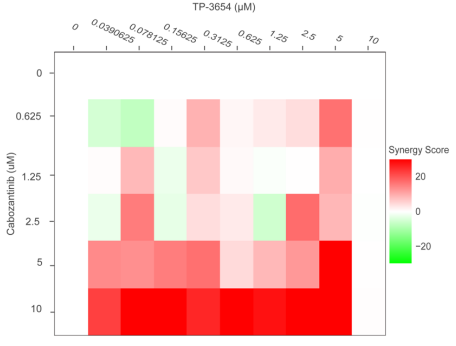

TP-3654 (μM)	Cabozantinib (μM)	Synergy Score
0.625	10	48.12
5	10	46.11
0.15625	10	41.29
2.5	10	35.64
5	5	31.95
0.078125	10	30.13
1.25	10	28.00
0.3125	10	25.52
0.0390625	10	22.49
2.5	2.5	17.31
0.3125	5	16.84
5	0.625	16.66
0.078125	2.5	15.46
0.15625	5	15.35
0.0390625	5	13.78
0.078125	5	13.23
2.5	5	12.16

Figure 5. Indirect and direct PIM inhibitors exert synergy when used in combination with VEGF inhibition in 786-O cells. Representative luminescent image of 786-O cells treated with cabozantinib and ruxolitinib in combination for 72 hours (left panel). Cell viability measured by Cell-Titer-Glo (CTG) assay and represented as % inhibition (left middle panel). Synergy scores calculated using SynergyFinder+ HAS formula (right middle panel) Scores greater than 10 indicate synergism (table) (A). Representative luminescent image of 786-O cells treated with cabozantinib and SGI-1776 in combination for 72 hours. Cell viability measured by CTG. Synergy scores indicated (B). Representative luminescent image of 786-O cells treated with cabozantinib and TP-3654 in combination for 72 hours. Cell viability measured by CTG. Synergy scores indicated (C).

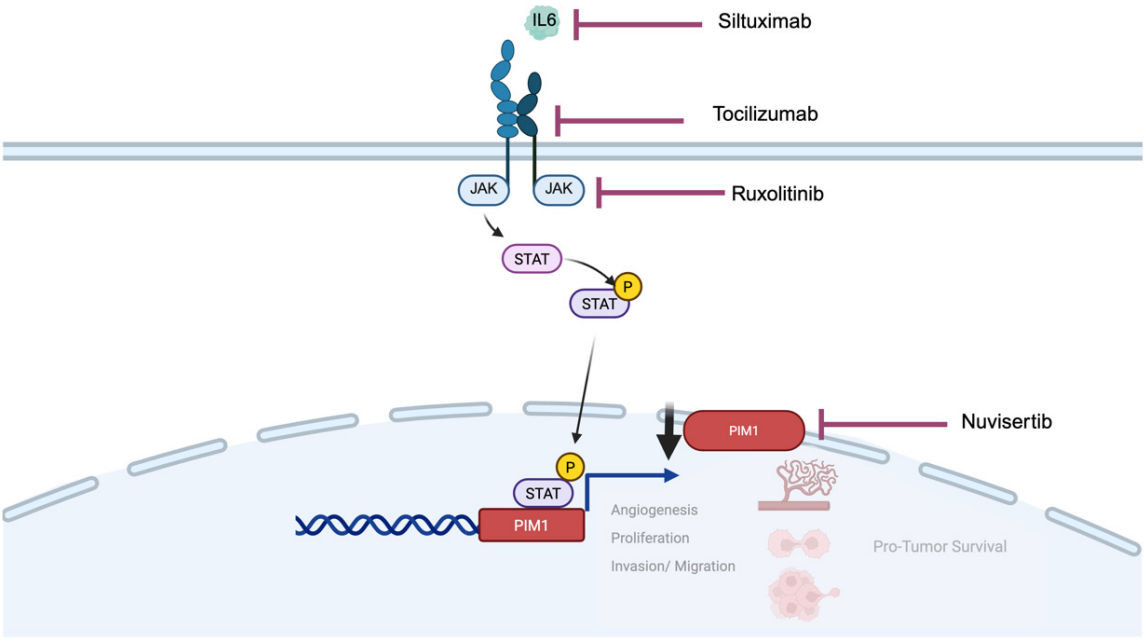

Figure 6. Graphical summary of a targetable IL-6/JAK/STAT/PIM axis in RCC. Agents listed are currently FDA approved (Siltuximab, Tocilizumab, Ruxolitinib) or have FDA Fast Tracked Designation (Nuvisertib/TP-3654). Created with BioRender.com.

high ccRCC. Additionally, *PIM1* expression or protein levels, or even serum IL-6 levels may simultaneously be evaluated as potential biomarkers for efficacy of IL6/JAK/STAT/PIM1 directed therapy. Here, we show that combinations of JAK (ruxolitinib) or PIM (SGI-1776, nuvisertib/TP-3654) inhibitors with VEGF inhibitors (cabozanitinib) act synergistically to reduce cell viability in PIM1 high 786-O cells. These strategies, such as using ruxolitinib in combination with cabozantinib, may offer increased benefit for *PIM1* high expressing ccRCC tumors. Both SGI-1776 and TP-3654 also show synergy with cabozantinib. However, targeting PIM1 directly in ccRCC is not immediately clinically feasible due to the lack of FDA approved selective direct PIM1 inhibitors. Nuvisertib (TP-3654) offers promising possibilities as it is currently in clinical trials for myelofibrosis and received FDA Fast Track Designation [58, 59]. *In vivo* studies are planned to verify the activity of combination therapies, particularly given the mechanism of action of cabozantinib.

An unexpected finding was that 769-P cells, despite having high levels of PIM1 protein, do not secrete IL-6. Treatment with ruxolitinib had no effect on PIM1 protein levels in 769-P cells. These data suggest that in 769-P cells there is a JAK-independent mechanism regulating PIM1 expression. Further studies are underway to elucidate the components of a putative alternative pathway, which we anticipate will reveal additional novel targets in ccRCC.

Also of interest is that PIM1 activity may be important in sarcomatoid RCC. We observed a trend towards worse survival in patients with *PIM1*-high sarcomatoid RCC. The low total number of patients in this cohort limits the statistical power and likely accounts for the lack of

statistical significance in OS outcomes in this cohort. The observed survival trend, however, is supported by a statistically significant increase in *PIM1* expression in metastatic sarcomatoid RCC tumors relative to primary sarcomatoid RCC tumors. Future studies will further examine the role of *PIM1* in sarcomatoid RCC, including a potential association between *PIM1* expression and overall survival.

In summary, PIM1 is a biomarker of poor prognosis and an attractive therapeutic target for ccRCC therapy. An upstream IL-6/JAK/STAT pathway influences *PIM1* expression in ccRCC. We are engaged in ongoing studies to elucidate the beneficial effects of targeting the IL-6/JAK/STAT pathway in the treatment of *PIM1*-high ccRCC. Future studies are aimed at further characterizing and interrogating the molecular mechanisms controlling PIM1 activity in RCC.

Acknowledgements

We thank our sources of funds that made this work possible (Kidney Cancer Association 2022 Trailblazer Award and NIH R25GM08-3270).

Disclosure of conflict of interest

W.S.E-D., Associate Editor-in-Chief at AJCR, was not involved in the review or decision-making of this manuscript.

Address correspondence to: Dr. Sheldon L Holder, Department of Pathology and Laboratory Medicine, Brown University, 70 Ship St, Providence, RI 02903, USA. E-mail: sheldon.holder@trinity-health.org

References

[1] Siegel RL, Kratzer TB, Wagle NS, Sung H and Jemal A. Cancer statistics, 2026. CA Cancer J Clin 2026; 76: e70043.

[2] Kase AM, George DJ and Ramalingam S. Clear cell renal cell carcinoma: from biology to treatment. Cancers (Basel) 2023; 15: 665.

[3] National Cancer Institute. (2026). Kidney and Renal Pelvis Cancer - Cancer Stat Facts. SEER. https://seer.cancer.gov/statfacts/html/kidrp.html.

[4] Rose TL and Kim WY. Renal cell carcinoma. JAMA 2024; 332: 1001.

[5] Iskandar AS, Zarrabi KK and Tester WJ. Renal cell carcinoma: entering the age of biomarkers. Can J Urol 2024; 31: 11921-11930.

[6] Nabi S, Kessler ER, Bernard B, Flaig TW and Lam ET. Renal cell carcinoma: a review of biology and pathophysiology. F1000Res 2018; 7: 307.

[7] Gkolfinopoulos S, Psyrri A and Bamias A. Clear-cell renal cell carcinoma - a comprehensive review of agents used in the contemporary management of advanced/metastatic disease. Oncol Rev 2021; 15: 530.

[8] Ganini C, Montanaro M, Scimeca M, Palmieri G, Anemona L, Concetti L, Melino G, Bove P, Amelio I, Candi E and Mauriello A. No time to die: how kidney cancer evades cell death. Int J Mol Sci 2022; 23: 6198.

[9] Kim E and Zschiedrich S. Renal cell carcinoma in von Hippel-Lindau disease-from tumor genetics to novel therapeutic strategies. Front Pediatr 2018; 6: 16.

[10] Jonasch E, Donskov F, Iliopoulos O, Rathmell WK, Narayan VK, Maughan BL, Oudard S, Else T, Maranchie JK, Welsh SJ, Thamake S, Park EK, Perini RF, Linehan WM and Srinivasan R; MK-6482-004 Investigators. Belzutifan for renal cell carcinoma in von Hippel-Lindau disease. N Engl J Med 2021; 385: 2036-2046.

[11] Xiang Y, Zheng G, Zhong J, Sheng J and Qin H. Advances in renal cell carcinoma drug resistance models. Front Oncol 2022; 12: 870396.

[12] Hah YS and Koo KC. Immunology and immunotherapeutic approaches for advanced renal cell carcinoma: a comprehensive review. Int J Mol Sci 2021; 22: 4452.

[13] Wang Y, Suarez ER, Kastrunes G, de Campos NSP, Abbas R, Pivetta RS, Murugan N, Chalbatani GM, D'Andrea V and Marasco WA. Evolution of cell therapy for renal cell carcinoma. Mol Cancer 2024; 23: 8.

[14] Bratu O, Mischianu D, Marcu D, Spinu D, Iorga L, Cherciu A, Balescu I, Bacalbasa N, Diaconu C, Savu C, Savu C and Anghel R. Renal tumor biomarkers (Review). Exp Ther Med 2021; 22: 1297.

[15] Gulati S and Vogelzang NJ. Biomarkers in renal cell carcinoma: are we there yet? Asian J Urol 2021; 8: 362-375.

[16] Pastore AL, Palleschi G, Silvestri L, Moschese D, Ricci S, Petrozza V, Carbone A and Di Carlo A. Serum and urine biomarkers for human renal cell carcinoma. Dis Markers 2015; 2015: 251403.

[17] Tan PH, Cheng L, Rioux-Leclercq N, Merino MJ, Netto G, Reuter VE, Shen SS, Grignon DJ, Montironi R, Egevad L, Srigley JR, Delahunt B and Moch H; ISUP Renal Tumor Panel. Renal tumors: diagnostic and prognostic biomarkers. Am J Surg Pathol 2013; 37: 1518-1531.

[18] Mahalingam D, Espitia CM, Medina EC, Esquivel JA 2nd, Kelly KR, Bearss D, Choy G, Taverna P, Carew JS, Giles FJ and Nawrocki ST. Target-

ing PIM kinase enhances the activity of sunitinib in renal cell carcinoma. Br J Cancer 2011; 105: 1563-1573.
[19] Small J, Washburn E, Millington K, Zhu J and Holder SL. The addition of abemaciclib to sunitinib induces regression of renal cell carcinoma xenograft tumors. Oncotarget 2017; 8: 95116-95134.
[20] Zhao B, Liu L, Mao J, Zhang Z, Wang Q and Li Q. PIM1 mediates epithelial-mesenchymal transition by targeting Smads and c-Myc in the nucleus and potentiates clear-cell renal-cell carcinoma oncogenesis. Cell Death Dis 2018; 9: 307.
[21] Blanco-Aparicio C and Carnero A. Pim kinases in cancer: diagnostic, prognostic and treatment opportunities. Biochem Pharmacol 2013; 85: 629-643.
[22] Warfel NA and Kraft AS. PIM kinase (and Akt) biology and signaling in tumors. Pharmacol Ther 2015; 151: 41-49.
[23] Tursynbay Y, Zhang J, Li Z, Tokay T, Zhumadilov Z, Wu D and Xie Y. Pim-1 kinase as cancer drug target: an update. Biomed Rep 2016; 4: 140-146.
[24] Zhang X, Song M, Kundu JK, Lee MH and Liu ZZ. PIM kinase as an executional target in cancer. J Cancer Prev 2018; 23: 109-116.
[25] Arrouchi H, Lakhlili W and Ibrahimi A. A review on PIM kinases in tumors. Bioinformation 2019; 15: 40-45.
[26] Panchal NK and Sabina EP. A serine/threonine protein PIM kinase as a biomarker of cancer and a target for anti-tumor therapy. Life Sci 2020; 255: 117866.
[27] Toth RK and Warfel NA. Targeting PIM kinases to overcome therapeutic resistance in cancer. Mol Cancer Ther 2021; 20: 3-10.
[28] Zhao Y, Aziz AUR, Zhang H, Zhang Z, Li N and Liu B. A systematic review on active sites and functions of PIM-1 protein. Hum Cell 2022; 35: 427-440.
[29] Lai L, Chen X, Tian G, Liang R, Chen X, Qin Y, Chen K and Zhu X. Clinical significance of Pim-1 in human cancers: a meta-analysis of association with prognosis and clinicopathological characteristics. Cancer Control 2022; 29: 10732748221106268.
[30] Brault L, Gasser C, Bracher F, Huber K, Knapp S and Schwaller J. PIM serine/threonine kinases in the pathogenesis and therapy of hematologic malignancies and solid cancers. Haematologica 2010; 95: 1004-1015.
[31] Nawijn MC, Alendar A and Berns A. For better or for worse: the role of Pim oncogenes in tumorigenesis. Nat Rev Cancer 2011; 11: 23-34.
[32] Narlik-Grassow M, Blanco-Aparicio C and Carnero A. The PIM family of serine/threonine kinases in cancer. Med Res Rev 2014; 34: 136-159.
[33] Choudhury R, Bahadi CK, Ray IP, Dash P, Pattanaik I, Mishra S, Mohapatra SR, Patnaik S and Nikhil K. PIM1 kinase and its diverse substrate in solid tumors. Cell Commun Signal 2024; 22: 529.
[34] Chen L, Mao W, Ren C, Li J and Zhang J. Comprehensive insights that targeting PIM for cancer therapy: prospects and obstacles. J Med Chem 2024; 67: 38-64.
[35] Qian KC, Wang L, Hickey ER, Studts J, Barringer K, Peng C, Kronkaitis A, Li J, White A, Mische S and Farmer B. Structural basis of constitutive activity and a unique nucleotide binding mode of human Pim-1 kinase. J Biol Chem 2005; 280: 6130-6137.
[36] Liang C and Li YY. Use of regulators and inhibitors of Pim-1, a serine/threonine kinase, for tumour therapy (review). Mol Med Rep 2014; 9: 2051-2060.
[37] Xu L, Chen X, Shen M, Yang DR, Fang L, Weng G, Tsai Y, Keng PC, Chen Y and Lee SO. Inhibition of IL-6-JAK/Stat3 signaling in castration-resistant prostate cancer cells enhances the NK cell-mediated cytotoxicity via alteration of PD-L1/NKG2D ligand levels. Mol Oncol 2018; 12: 269-286.
[38] Luszczak S, Kumar C, Sathyadevan VK, Simpson BS, Gately KA, Whitaker HC and Heavey S. PIM kinase inhibition: co-targeted therapeutic approaches in prostate cancer. Signal Transduct Target Ther 2020; 5: 7.
[39] Block KM, Hanke NT, Maine EA and Baker AF. IL-6 stimulates STAT3 and Pim-1 kinase in pancreatic cancer cell lines. Pancreas 2012; 41: 773-781.
[40] Gao X, Liu X, Lu Y, Wang Y, Cao W, Liu X, Hu H and Wang H. PIM1 is responsible for IL-6-induced breast cancer cell EMT and stemness via c-myc activation. Breast Cancer 2019; 26: 663-671.
[41] Hirano T. IL-6 in inflammation, autoimmunity and cancer. Int Immunol 2021; 33: 127-148.
[42] Gudbrandsdottir G, Aarstad HH, Bostad L, Hjelle KM, Aarstad HJ, Bruserud O, Tvedt THA and Beisland C. Serum levels of the IL-6 family of cytokines predict prognosis in renal cell carcinoma (RCC). Cancer Immunol Immunother 2021; 70: 19-30.
[43] Meza KS, Seymour K and Holder SL. Abstract 627: IL-6 signaling via JAK/STAT axis influences PIM1 expression in renal cell carcinoma. Cancer Research 2024; 84: 627.
[44] Meza KS, Seymour K, Graff SL, Nabhan C, Elliott A and Holder SL. IL-6 and PIM1 expression in renal cell carcinoma. J Clin Oncol 2024; 42: 470.

[45] Cerami E, Gao J, Dogrusoz U, Gross BE, Sumer SO, Aksoy BA, Jacobsen A, Byrne CJ, Heuer ML, Larsson E, Antipin Y, Reva B, Goldberg AP, Sander C and Schultz N. The cBio cancer genomics portal: an open platform for exploring multidimensional cancer genomics data. Cancer Discov 2012; 2: 401-4.

[46] Gao J, Aksoy BA, Dogrusoz U, Dresdner G, Gross B, Sumer SO, Sun Y, Jacobsen A, Sinha R, Larsson E, Cerami E, Sander C and Schultz N. Integrative analysis of complex cancer genomics and clinical profiles using the cBioPortal. Sci Signal 2013; 6: pl1.

[47] Chandrashekar DS, Karthikeyan SK, Korla PK, Patel H, Shovon AR, Athar M, Netto GJ, Qin ZS, Kumar S, Manne U, Creighton CJ and Varambally S. UALCAN: an update to the integrated cancer data analysis platform. Neoplasia 2022; 25: 18-27.

[48] Chandrashekar DS, Bashel B, Balasubramanya SAH, Creighton CJ, Ponce-Rodriguez I, Chakravarthi BVSK and Varambally S. UALCAN: a portal for facilitating tumor subgroup gene expression and survival analyses. Neoplasia 2017; 19: 649-658.

[49] Deng YT, You J, He Y, Zhang Y, Li HY, Wu XR, Cheng JY, Guo Y, Long ZW, Chen YL, Li ZY, Yang L, Zhang YR, Chen SD, Ge YJ, Huang YY, Shi LM, Dong Q, Mao Y, Feng JF, Cheng W and Yu JT. Atlas of the plasma proteome in health and disease in 53,026 adults. Cell 2024; 188: 253-271, e7.

[50] Subramanian A, Tamayo P, Mootha VK, Mukherjee S, Ebert BL, Gillette MA, Paulovich A, Pomeroy SL, Golub TR, Lander ES and Mesirov JP. Gene set enrichment analysis: a knowledge-based approach for interpreting genome-wide expression profiles. Proc Natl Acad Sci U S A 2005; 102: 15545-15550.

[51] Liberzon A, Birger C, Thorvaldsdottir H, Ghandi M, Mesirov JP and Tamayo P. The Molecular Signatures Database (MSigDB) hallmark gene set collection. Cell Syst 2015; 1: 417-425.

[52] Raudvere U, Kolberg L, Kuzmin I, Arak T, Adler P, Peterson H and Vilo J. g:Profiler: a web server for functional enrichment analysis and conversions of gene lists. Nucleic Acids Res 2019; 47: W191-W198.

[53] Ianevski A, Giri AK and Aittokallio T. SynergyFinder 3.0: an interactive analysis and consensus interpretation of multi-drug synergies across multiple samples. Nucleic Acids Res 2022; 50: W739-W743.

[54] Zheng S, Wang W, Aldahdooh J, Malyutina A, Shadbahr T, Tanoli Z, Pessia A and Tang J. SynergyFinder Plus: toward better interpretation and annotation of drug combination screening datasets. Genomics Proteomics Bioinformatics 2022; 20: 587-596.

[55] Brooks SA, Brannon AR, Parker JS, Fisher JC, Sen O, Kattan MW, Hakimi AA, Hsieh JJ, Choueiri TK, Tamboli P, Maranchie JK, Hinds P, Miller CR, Nielsen ME and Rathmell WK. ClearCode34: a prognostic risk predictor for localized clear cell renal cell carcinoma. Eur Urol 2014; 66: 77-84.

[56] Macdonald A, Campbell DG, Toth R, McLauchlan H, Hastie CJ and Arthur JS. Pim kinases phosphorylate multiple sites on Bad and promote 14-3-3 binding and dissociation from Bcl-XL. BMC Cell Biol 2006; 7: 1.

[57] Morishita D, Katayama R, Sekimizu K, Tsuruo T and Fujita N. Pim kinases promote cell cycle progression by phosphorylating and down-regulating p27Kip1 at the transcriptional and posttranscriptional levels. Cancer Res 2008; 68: 5076-5085.

[58] Rein LAM, El Chaer F, Yuda J, Shimoda K, McCloskey J, Takami A, Haque T, Ichii M, Shirane S, Fukaya M, Scandura JM, Bradley T, Vachhani P, Tabayashi T, Green S, Cheung S, Bose P, Khurana S, O'Connell CL, Amanam I, Ross DM, Kabir S, Seki M, Wade M, Peddagali V, Li Z, Shah J and Rampal RK. Phase 1/2 study of TP-3654, a selective PIM1 kinase inhibitor: preliminary data showed clinical activity and cytokine reductions in relapsed/refractory myelofibrosis patients. Blood 2023; 142: 626.

[59] Sumitomo Pharma America Announces that Nuvisertib (TP-3654) Has Received FDA Fast Track Designation for the Treatment of Myelofibrosis. (2025). Sumitomo Pharma America Newsroom. https://news.us.sumitomo-pharma.com/2025-06-12-Sumitomo-Pharma-America-Announces-that-Nuvisertib-TP-3654-Has-Received-FDA-Fast-Track-Designation-for-the-Treatment-of-Myelofibrosis.